AN EXPERIMENTAL STUDY FOR INTERACTION FLOW BETWEEN SHOCK WAVE AND TURBULENT BOUNDARY LAYER

Li Suxun Shi Yueding Cai Hanlong
Beijing Institute of Aerodynamics
P.O.Box 7215 Beijing China

Abstract

The typical interactive flows between shock wave and boundary layer are studied experimentally in a hypersonic wind tunnel. The free stream Mach number is 5, and Reynolds number per meter is 5.7×10^7 at test section. A set of shock generators are used to get three dimensional shock wave, and it induces the turbulent boundary-layer separation and reattachment on a received flat plate. In this interactive region, the static pressure, fluctuating pressure and heat flux distributions along the centre line of received plate have been measured under the same test conditions. The visualizations of schlieren photograph in space and oil flow patterns on the surface show the separated region. By comparing the visualization results with measurement data the special positions at the static pressure and heat flux distributions can be marked.

All the results give overall flow features for three dimensional separated flows. The effects of shock wave strength, some unsteady behaviors and the correlations between static pressure and heat transfer are discussed.

Nomenclature

H	distance between shock generator and received plate
M	Mach number
P	static pressure
P'	fluctuating pressure
q	dynamic pressure or heat flux
Re	freestream unit Reynolds number
T	temperature
t	time
X	co-ordinate parallel to the tunnel axis measured from nozzle exit.
Y	co-ordinate normal to the x axis at received plate
α	geometric shock generator incidence
δ	boundary layer thickness at plane centre before interaction
β	shock wave angle

Subscripts:

∞	freestream conditions
w	on the received plane

This work is supported partially by National Nature and Science Foundation of China.

I. Introduction

One kind of complex flow in gas dynamics is the separated (and reattached) flow, which is induced by the interaction between shock wave and boundary layer. When the shock strength is strong enough, it can cause flow separation and change the overall flow field. It is important to determine the influence region and load distributions including static and fluctuating pressure as well as heat transfer features for aircraft and space flight designs and other aviation engineering problems.

During the past years, many kinds of interactive flows are investigated in transonic, supersonic and hypersonic flows. The typical interaction models are contained such as flat plate/wedge, incident shock with surface, cone/flare, at transonic airfoil, in diffusers of centrifugal compressors or wind tunnels, at centrebody inlets and in turbomachinery cascades. Two dimensional shock wave/boundary layer interactions have been studied extensively, both experimentally and theoretically, over a wide range of conditions [1,2,3,4,5], but in practice nearly all interactions occurring on high speed vehicles are either fully three dimensional or display some degree of three dimensionality.

The significant differences between two and three dimensional interaction flows have been presented [4,6,7,8]. The interactive flow patterns in three dimensional are more complex compared with two-dimensional flow field. Some problems are still not understood. Many results published concentrate on static pressure characteristics and partially on fluctuating pressure behavior at interaction region in transonic and supersonic flows [9,10]. The heat transfer problems require more intentions for space vehicle design in hypersonic flows [11,12].

In recent, more complex interactive flow are studied such as shock/vortex interaction and double shock/boundary layer interactions [13,14].

In this paper some interactive flows between three dimensional shock wave and turbulent boundary layer are studied experimentally in the blowdown hypersonic wind tunnel of BIA [10,12,15].

A shock wave generator is used to get a three-dimensional shock wave which is incoming to a received flat plate, then the turbulent boundary layer flow is separated and reattached on the surface. In this interactive region, the static pressure, fluctuating pressure and heat flux distributions are measured by several techniques. The schlieren photographs and oil coating patterns show the shock wave structures in the space and separation region on the surface, respectively. It shows the complex three dimensional separated flows. There are five shock generators with different leading edge. All test works are carried out in same test conditions.

II. Experimental Program

2.1 Wind tunnel and test conditions

The experimental study are carried out in the hypersonic blowdown wind tunnel of BIA. This wind tunnel has a working section $17cm \times 17cm$.

In this study all test cases have same free stream conditions, stagnation pressure and temperature are 3.5 MPa and 430K corresponding to a free stream Mach number of 5 and unit Reynolds number of $5.7 \times 10^7 M^{-1}$. The models are at cooling wall condition. A temperature ratio of wall and stagnation is 0.65-0.7. The test section with unreflection boundary is covered by a big tank room (stagnation room) to keep the pressure uniform around the test section.

2.2 Model Configurations

An experimental model consists of two parts: One is a shock wave generator and other is a received flat plate.

A set of generators with five nose shapes is used for changed the incident shock wave strength on the bottom of test section for pressure and heat flux measurements respectively. In each test case, one of the generators and one received flat plate are installed in the test section, shown in Figure 1.

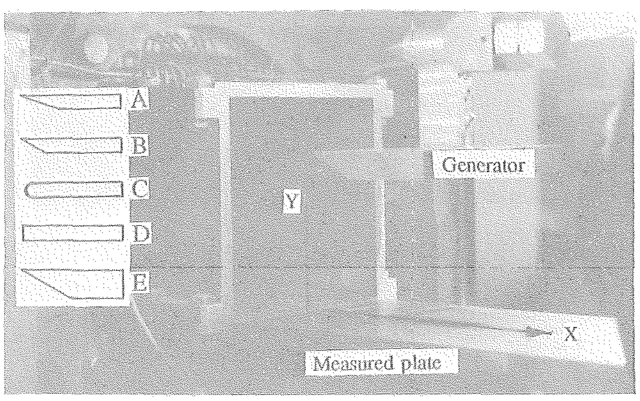

The free stream Mach number is 5, and Reynolds number per meter is 5.7×10^7 at test section.

Figure 1. Schematic Experimental Configuration and Coordinate System

X coordinate is along with the bottom and the original point is put on nozzle exit, and Y coordinate is normal to X. Shock wave generator is a wedge-plate (or a blunt nose-plate), it can be moved in the normal direction (Y), when the test flow has been built, a three dimensional shock wave occurs from the leading edge of the generator, then the shock wave is incident to the measurement flat plate. Before testing the generator is kept in the tank room.

2.3 Test program and instruments

The schlieren photos are taken for each case, and the oil flow techniques have been special made for partial cases. The mean static pressure are measured by 36 strain gage transducers. Two types of transducers, condenser mini-microphone B & K 4136 and strain gage transducer are mounted under the surface to measure fluctuating wall pressure. All data are recorded by recorder and reduced by SM-2100 B signal Analyzer, as fluctuating pressure sample chart. For obtaining the heat flux features, a received plate is made by thin steel flat plate where 25 thermocouples are mounted along the centre line, the measurement position are listed in Table 2. The thermo couples are special made with 1mm size, and the surface temperatures variated with times are measured, as in a following chart.

Pressure Sample Chart

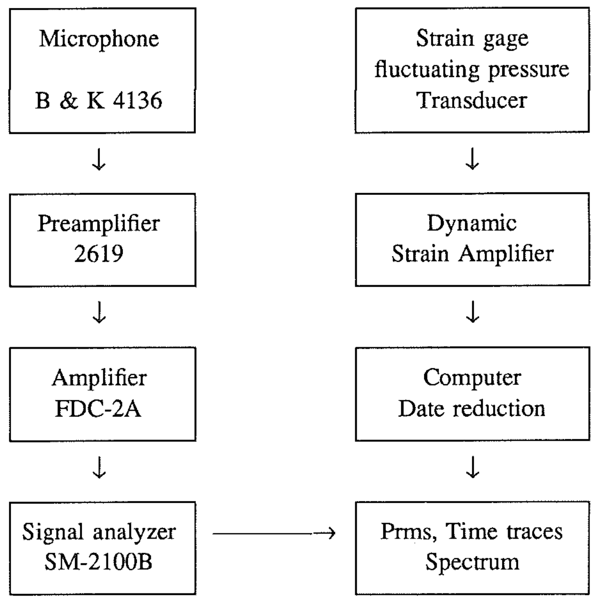

Heat Flux Sample Chart

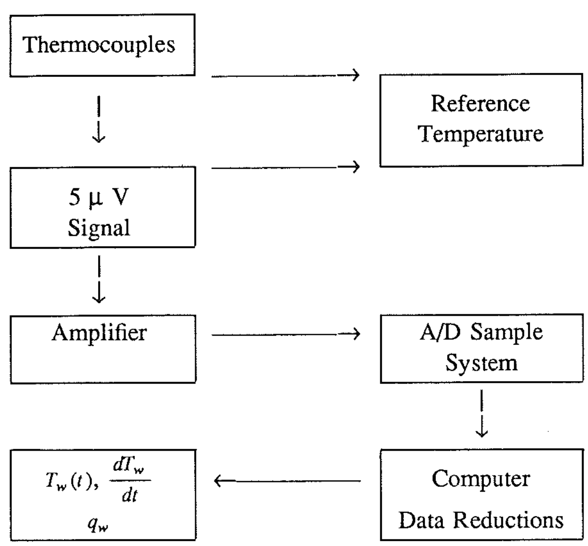

2.4 Test cases

There are five generators with A. B. C. D. E leading edge forms, shown in Figure 1, each one of them is set up in the test section for one case, so all test cases (C) are listed in Table 1.

Table 1 Test cases listing

C / Hmm / L.E	1	2	3	4
A		100.5	88	76
B.C.D	129.5	100.5	88	76
E	127.5	106.5	88	

The measurement positions of static pressure, fluctuating pressure and heat flux are given in Table 2.

Table 2 mean and fluctuating wall pressure as well as heat flux measurement positions

MEAN PRESSURES	NO(CH)	1->6		7->31		32->36	
	Xmm	30->90		103->247		260->320	
FLUCT. PRESSURE	NO(CH)	1	2	3	4	5	6
	Xmm	139	151	163	187	199	211
HEAT FLUX	NO(CH)	1 ------>25					
	Xmm	115 ------>235					

III. Experimental Techniques and Results

3.1 Visualizations

As mentioned above, during the tests, the schlieren photographs are taken to diagnose the flow field for each case, and oil flow techniques utilized to show skin friction lines on the wall partially. It shows that a simple incident shock wave (IS) is incoming to a thick turbulent boundary layer, then flow separated from the surface. The separation position is located in front of incident impact point, near the separation line the boundary layer thickness is increasing suddenly, so that a separated shock wave (SS) occurs at upstream of IS. The incident shock is end at sound line in flow field close to surface, the shock can not arrive to the surface, and reflects from sound boundary to downstream direction. Around the separated region the expansive waves (EW) and reflected weak shock system (RS) are formed. Behind RS system the separated flows are reattached [10,15]. A schlieren photograph is given in Figure 2.

Usually the convergent or divergent friction line is corresponding to separated or reattached line on the surface, respectively. A typical skin friction pattern is visualized by Titanium and carbon/vacuum pump oil coating in Figure 3,

Generator

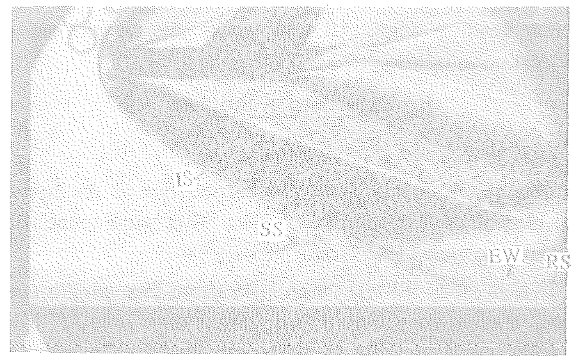

IS. Incident Shock SS. Separated Shock
RS. Reflected Shock EW. Expensive Waves

Figure 2. Schlieren Photograph and Shock wave System

S.R. Separated Region R.R. Reattached Region

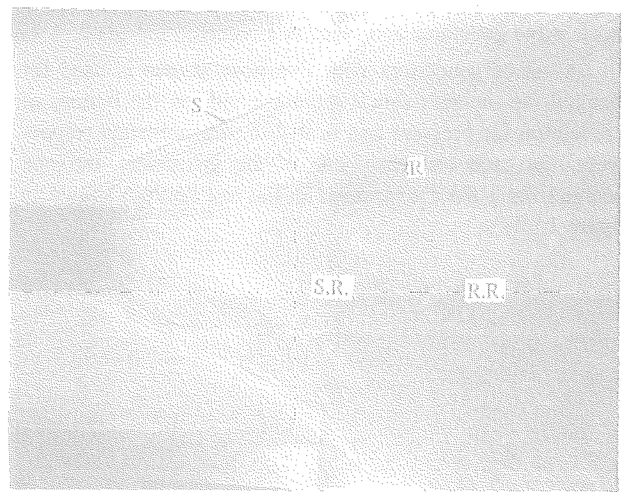

Figure 3. Oil flow Pattern and Divided Region

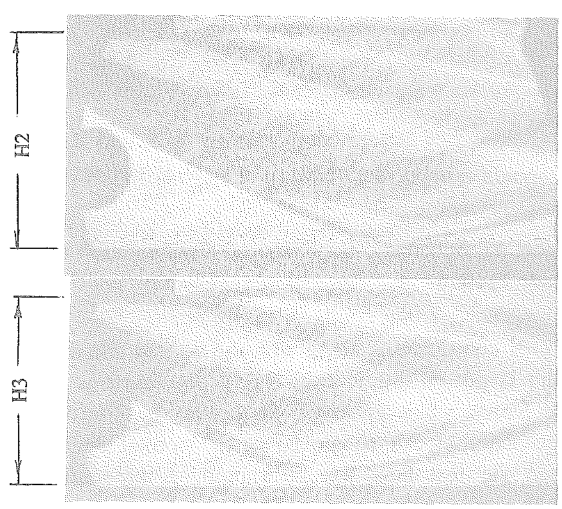

Figure 4. Shock Strength Varies With H

it shows that some friction lines with U turn form. For one fixed generator which is set up in test section, if the distance H is decreasing, the shock strength becomes strong at ideal impact point corresponding to a large angle of shock wave (β). In this case, the separated region moves to upstream and the influence region is extend to all around, in figure 4.

For two cases (A,D) the shock wave angles in the symmetric plane of flow field are measured without boundary layer effect, in Figure 5.

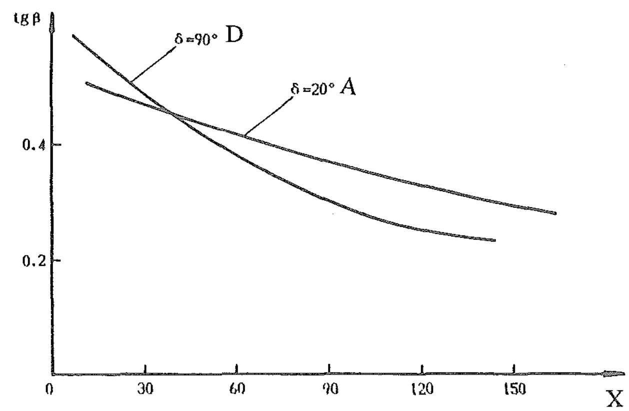

Figure 5. Shock Wave Angles in Symmetric Plane for Case A and D

3.2 Static Pressure Characteristics

The mean static pressures are measured by strain gage transducers along the center line of received plate for all cases in Table 1. The mean flow phenomena are exposed by visualization pictures such as in Figure 2, 3 and 4, dependent on that we marked some positions at the static pressure distributions as in Figure 6, in which there are four cases (B-1, B-2, B-3, B-4). For each case, we can find five special positions as following:

R_1	:	the first pressure rising point corresponding to upstream influence line
S	:	Separation point
R_2	:	the second pressure rising point in the separated region
R	:	reattached point
R_m	:	maximum pressure point at reattached flow

They are marked respectively. The reattached point R is located between R_2 and R_m, a set of reflect shocks occurred around this point. The static pressures p_w on the surface are normalized by upstream pressure P_∞.

In figure 7, the static pressure distributions produced by five noses of generators indicate that if the shock strength at ideal reflect point is increasing, then

i) the range of separated region is expanded

ii) the value of P_w max (at R_m) is increasing

iii) a plateau region of pressure in separated flows is exist,

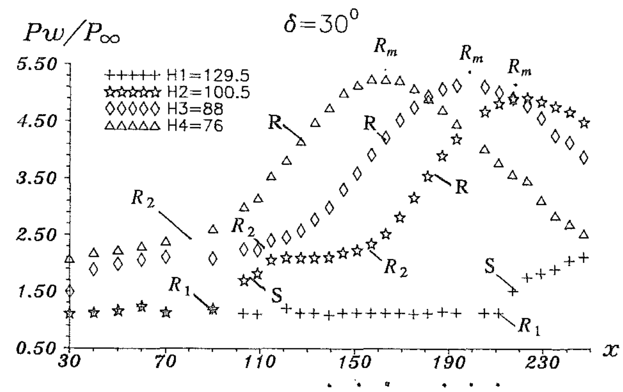

Figure 6 Static pressure distributions for case B, δ=30°

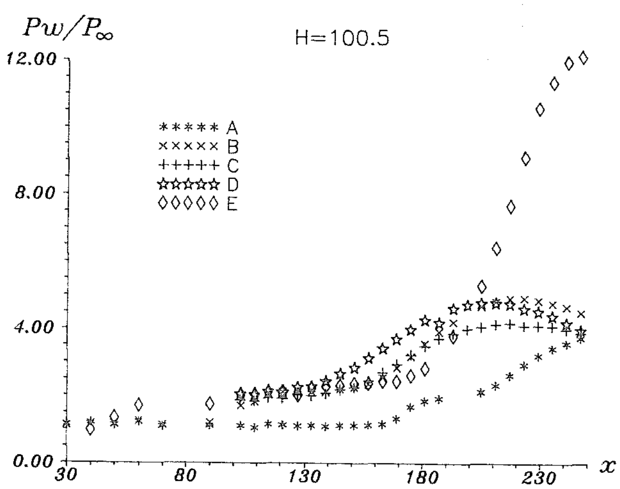

Figure 7 Static pressure distributions for cases A-2, B-2, C-2, D-2, E-2 at same H conditions

which is similar with two dimensional flow, the ratio of P_w/P_∞ is about 2

iv) near the separated point (S) the ratio of P_w/P_∞ is between 1.5~1.7

v) the dP_w/dx close to S point is a important factor.

In present study, the incident angle of shock wave means shock strength.

3.3 Fluctuating pressure and unsteady flow features

In order to insure structural integrity and reliability requirements of high speed vehicles it is necessary to know the interacted flow not only for steady flow but also for unsteady flow features.

There are six channels to take the fluctuating signal from fluctuating pressure transducers which are mounted on the received plate according to the positions in Table 2.

In same test case, six channels can record signals of different positions in a interactive flow. For example, in case B-1 a generator B is set up at H = 129.5mm height corresponding to channels 1->5, located in front of S point, only channel 6 close to point R_1, for the all cases, each channel stands in different region of the interactive flows as listed in Table 3.

Table 3 Various flow status Corresponding to channel Numbers

Channel	1	2	3	4	5	6
Case B-1	without separation					close to R1
Case B-2	Separation region		Reattached flow			
Case B-3	Separation region		Reattached flow			
Case B-4	Reattached flow					

Table 4 Prms of channel 3 for all case B

Case	B-0	B-1	B-2	B-3	B-4
Hmm	150	100	88	76	65
Prms/q	.0146	.0148	.0189	.0188	.0180
Status	upstream of S Point		separated region		reattached region

Many functions of data analysed are made by SM-2100 B signal Analyzer. One of them is the Root-mean-square of fluctuating pressure Prms which is obtained and normalized by dynamic pressure q, a dimensionless P_{rms}/q at channel 3 is shown in Table 4, it shows the results of peak value of P_{rms}/q are not found in this time, at separation region and near reattached flow region the P_{rms}/q are close to 2 percent.

B-1

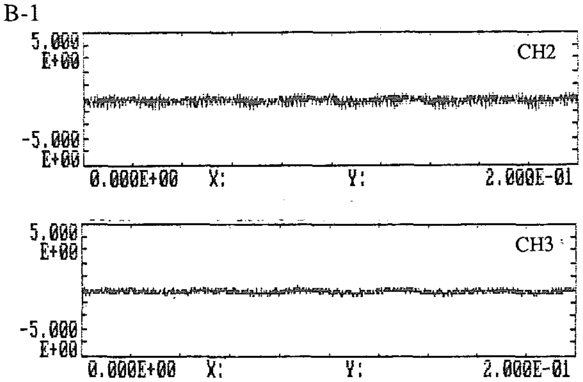

B-2

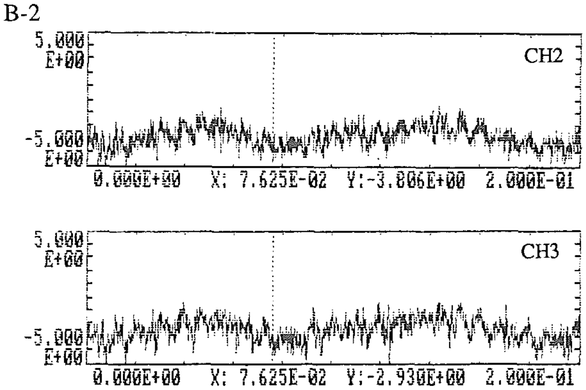

B-4

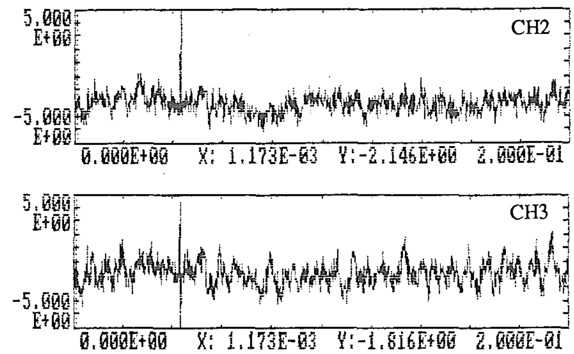

Figure 8 The time traces of signals at CH2, CH3 for B-1, B-2, B-4

B-1

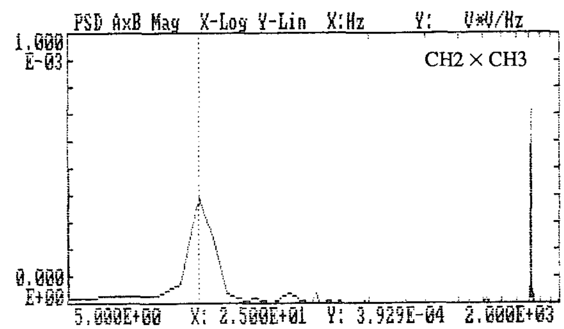

B-2

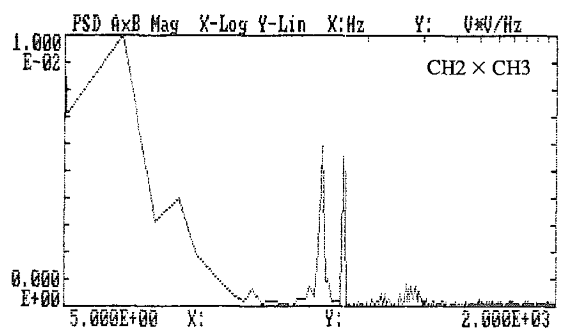

B-4

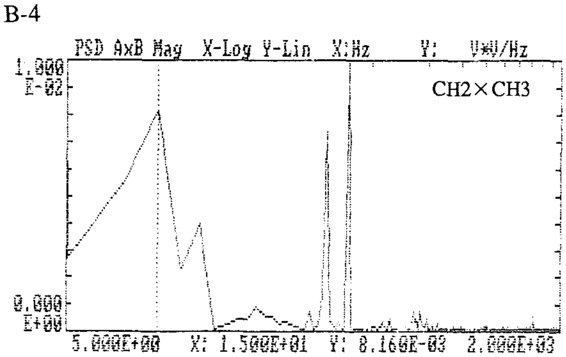

Figure 9 Correlation power density spectrum between CH2, CH3

The time traces of fluctuating pressure signals at CH2 and CH3 are recorded and plotted in Figure 8 for case B-1, B-2 and B-4, the flows pass by the measured positions 2 and 3 in different status as Table 3. The time traces express that for case B-1 both signals are in smaller perturbations, which is taken in front of S point, for case B-2 the signals taken in separated region are enhanced and some low frequence oscillations are found in same step of both positions, for case B-4 both of time traces keep enhanced signals, but the lowest frequence is changed a little.

In Figure 9 under same test conditions with Figure 8, the correlation power density spectrum between CH 2 and CH 3 is built, the low frequences f_1, f_2, f_3, f_4 are identified as Table 5.

Table 5 Correlation Coefficient and frequences

Correlation Channel	2 × 3			2 × 5
Case	B-1	B-2	B-4	B-2
f_1	25	10	15	10
f_2		20		25
f_3		115	115	115
f_4		150	150	150
Correlation coefficient in space	.48	.98	.623	.88
Channel Location	Upst. of S.P	Separ. region	Down. of R.P	CH2 in S.R CH5 in R.R

These results indicate that in separated region and near downstream the correlation coefficients of either CH 2 with CH 3 or CH 2 with CH 5 are close to 1, that means the ensemble flow motions with low frequence occur at interacted region.

In all cases, the lowest frequences are found from 7hz to 20hz, the higher frequences are more than several hundred. In ref (10) two pictures which are taken by high speed camera with time interval 0.39 μ second are compared and shown that the incident shock wave oscillation in shadograms, therefore we considered that the interactive flows are highly unstable.

All the fluctuating data are taken in 0.2 second and frequence branch of 2000hz for sample analysis.

3.4 Heat transfer measurements

Before the test flow built, the generator was setup in the tank room and the received plate should be covered by a soft protection curtain for keeping constant ratio of surface temperature to the flow stagnation temperature. The soft curtain is made by leather, which can be moved quickly to back area of the measured plate after the test flow built.

During the test, the surface temperatures with time $T_w(t)$ are recorded, dependent on one dimensional heat con-

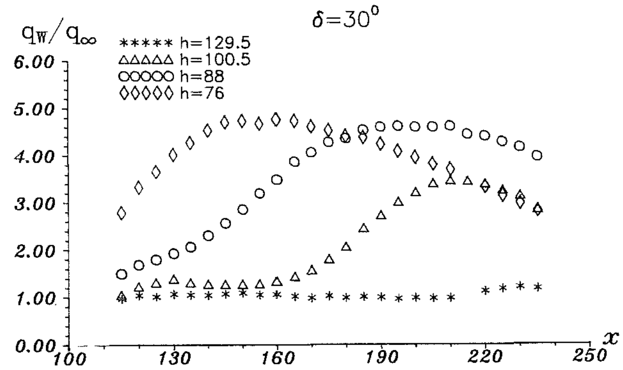

Figure 10 Heat flux distributions for case B

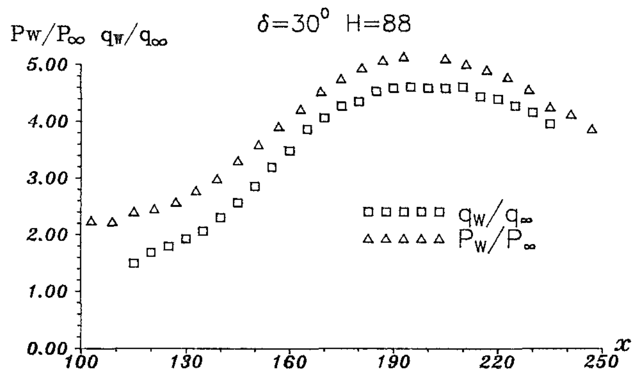

Figure 11 Comparison of static pressure and heat flux distributions

duction model the measured data are reduced. The local heat flux q_w for each point is expressed as

$$q_w = \delta_m \, C_m \, \delta_s \, \frac{dT_w}{dt}$$

Where δ_m and C_m are the density and heat absorption capacity of steel, respectively, δ_s is the thickness of measured plate.

All of these can be determined before test, except $\frac{dT_w}{dt}$ is taken from test data for every thermocouple. The $q_w(x)$ distributions are shown in Figure 10, which are similar with static pressure distributions in same test conditions in Figure 6. and in Figure 11, both P_w/P_∞ and $q_w/q_{w\infty}$ are put together for comparison, it has same x position at peak value of P_w and q_w for each case. A few investigations have been mentioned about similar results in different interactive flows [11].

In order to determine the level and location of maximum load from one to another, it is necessary to build a correlation between peak values of P_w/P_∞ and $q_w/q_{w\infty}$. For example, if we have known the peak of P_w/P_∞ and its location on the surface, then the peak of $q_w/q_{w\infty}$ can be predicted conveniently. Dependent on present data there is a correlation between both of them which are taken from more than 10 cases as following

$$\left(\frac{q_w}{q_{w\infty}}\right)_{max} = \left(\frac{P_w}{P_\infty}\right)_{max}^{0.92\pm0.045}$$

IV. Conclusions

In this study, the experiments are carried out in hypersonic wind tunnel with several techniques, the visualization and measurement results give some information on three dimensional interacted separation flows between incident shock wave and turbulent boundary layer.

The main conclusions are as following:

1. The three dimensional separated flows induced by shock wave are more complex than two dimensional flows, the schlieren photos and shadograms only show the flow field on symmetric plane and oil flow patterns expose the skin friction lines such as convergent line, divergent line and U turn line corresponding to separated and reattachment flows.

2. The range of separated flow depends on the incident shock strength of the impact point at surface similar with two dimensional flow.

3. The mean static pressure distributions express that the special positions on the wall and the plateau pressures in separated flow are about 2 of P_w/P_∞. At the S point, the P_w/P_∞ is about 1.5~1.7 for present study.

4. The unsteady flow features are described in influence region. The Prms, power density spectrum and correlations of space and time are obtained based on fluctuating pressure data. The low frequence oscillations of separated flow occur as ensemble motions.

5. The heat flux distributions in interactive region are similar with static pressure distributions, and the relationship between both of peak values is built based on present experimental data.

References

[1] Settles, G.S., Bogdonoff, S.M., and Vas, I.E., Incipient Separation of a Supersonic Turbulent Boundary Layer at High Reynolds Numbers AIAA Journal, Vol.14, No.1, Jan, 1976. pp 50-56.

[2] Lilbur, L.H. Jr., Theoretical Developments in Supersonic Separated flows ADA-13882, 1975.

[3] Christophel, Robert. G., Two Dimensional Shock Wave Boundary Layer Interactions ADA 16469, 1975.

[4] Chang, P.K., Separation of Flow Pergamon Press, First Edition 1970. Liu , X., and Squire, L.C.

[5] An Investigation of Shock/Boundary-Layer Interaction on Curved Surfaces at Transonic Speeds J. Fluid Mach. (1988), Vol.187, 467-486.

[6] Oskam, S.M., Vas, I.E., and Bogdonoff, S.M., Mach 3 Oblique Shock Wave/Turbulent Boundary Layer Interactions in Three Dimensions, AIAA paper 76-336.

[7] Dolling, D.S., Cosad, C.D., and Bogdonoff, S.M., Three-Dimensional Shock Wave Turbulent Boundary Layers Interactions-A Parametric Study of Blunt Fin-Induced Flows , AIAA paper 78-159.

[8] Settles, G.S., and Dolling, D.S., Swept Shock-Wave/Boundary-Layer Interaction Tactical Missile Aerodynamics, Edited by Hemsch, M.J., and Nielsem, J.N.

[9] Bogdonoff, S.M. The Structure and Control of Three-Dimensional Shock Wave Turbulent Boundary Layer Interactions, AIAA 187642, 1987.

[10] Li S.X., Shi Y.D., Cai H.L. and Chen G.L. A Study of Fluctuating wall Pressure Measurements on Shock Wave/Turbulent Boundary Layer Interactions in Hypersonic Flows, Engineering Turbulence Modelling and Experiments, Edit by W.Rodi and E.N Ganik Elsevier 1990, 603-610.

[11] Holden M.S., A Review of Aerothermal Problems Associated with Hypersonic Flight , AIAA paper 86-0267.

[12] Li S.X., Shi Y.D. and Cai H.L. A Study of Hypersonic Separation Flow on Heat Transfer Features, will be Published Fifth Asian Congress of Fluid Mechanics, Aug. 1992, Korea.

[13] Copening, G., Anderson, J., Numerical Solutions to Three-Dimensional Shock Wave/Vortex Interaction at Hypersonic Speeds, AIAA 89-0674.

[14] Batcho, P.F., Ketchum, A.C., Bogdonoff, S.M., and Fernando, E.M., Preliminary Study of the Interactions Caused by Crossing Shock Waves and a Turbulent Boundary Layer, AIAA paper 89-0359.

[15] Shi, Y.D., Li, S.X. and Cai, H.L., A Visualization Investigation of Near Wall Flow Field in Hypersonic Flow, to be published in The 2nd China-Japan Symposium on Visualization, 1992, China.